Multiphase phase field theory for temperature- and stress-induced phase transformations

Valery I. Levitas[1,*] and Arunabha M. Roy[2]

[1]*Iowa State University, Departments of Aerospace Engineering, Mechanical Engineering, and Material Science and Engineering, Ames, Iowa 50011, USA*

[2]*Iowa State University, Department of Aerospace Engineering, Ames, Iowa 50011, USA*

(Received 5 December 2014; revised manuscript received 1 May 2015; published 21 May 2015)

Thermodynamic Ginzburg-Landau potential for temperature- and stress-induced phase transformations (PTs) between n phases is developed. It describes each of the PTs with a single order parameter without an explicit constraint equation, which allows one to use an analytical solution to calibrate each interface energy, width, and mobility; reproduces the desired PT criteria via instability conditions; introduces interface stresses; and allows for a controlling presence of the third phase at the interface between the two other phases. A finite-element approach is developed and utilized to solve the problem of nanostructure formation for multivariant martensitic PTs. Results are in a quantitative agreement with the experiment. The developed approach is applicable to various PTs between multiple solid and liquid phases and grain evolution and can be extended for diffusive, electric, and magnetic PTs.

I. INTRODUCTION

One of the unresolved problems of the phase field approach (PFA) for PTs is a noncontradictory description of PTs between an arbitrary number of phases. One of the directions is related to the description of PTs between the austenite (A) and any of the n martensitic variants M_i and between martensitic variants. [1] It is described with the help of n independent order parameters η_i, each for every $A \leftrightarrow M_i$. This approach was significantly elaborated in Refs. [2,3] by imposing additional physical requirements to the Landau potential. In particular, the desired PT conditions for $A \leftrightarrow M_i$ and $M_j \leftrightarrow M_i$ PTs follow from the material instability conditions. Also, the thermodynamically equilibrium transformation strain tensor is stress- and temperature-independent, as in crystallographic theories. Each order parameter η_i encodes variation of atomic configuration along the $A \leftrightarrow M_i$ transformation path; it is equal to 0 for A and 1 for M_i. In Refs. [2,3] and here η_i is unambiguously related to transformation strain through some polynomial [see Eqs. (3) and (8)].

This theory was generalized for large strain and lattice rotations, [4,5] and interface stresses consistent with a sharp interface approach have been introduced for A-M_i interfaces. [5–7] However, the description of M_i-M_j is still not satisfactory. The $A \leftrightarrow M_i$ PT is described by a single order parameter η_i, and analytic solutions for η_i for nonequilibrium interfaces [3,5–7] allow one to calibrate interface energy, width, and mobility, as well as the temperature dependence of the stress-strain curve. At the same time, at a M_i-M_j interface η_i and η_j vary independently along some transformation path in the $\eta_i - \eta_j$ plane connecting M_i ($\eta_i = 1$ and $\eta_j = 0$) and M_j ($\eta_i = 0$ and $\eta_j = 1$); see Fig. 1.

The interface energy, width, and mobility have an unrealistic dependence on temperature, stresses, and a number of material parameters which cannot be determined analytically. Consequently, one cannot prescribe the desired M_i-M_j

interface parameters, and the expression for M_i-M_j interface stresses cannot be strictly derived [5,6].

Other n-phase approaches are based on introducing $n + 1$ order parameters η_i obeying constraint $\sum \eta_i = 1$, similar to concentrations [8–10,13]. The idea is that each of the PTs should be described by a single order parameter; then interface parameters can be calibrated with the help of the analytical solution. However, a single constraint cannot ensure this, and, in general, an undesired in this community third phase often appears at the interface between two phases. PT criteria in terms of instability conditions are not considered. In Ref. [10] special conditions are imposed for a three-phase system that guarantee that the third phase can never appear at the interface between two phases. This created some artifacts in the theory (e.g., the necessity of equal kinetic coefficients for all PTs). All homogeneous phases are stable or metastable independent of the driving force (temperature); i.e., thermodynamic instability, which is the source of the PT criteria, is impossible. On the other hand, for different materials and conditions, the third phase is observed in experiments [11] and conditions when it is present or not are found within more advanced models [12]. Some drawbacks of imposing constraint with the help of Lagrangian multipliers are presented and overcame in Ref. [13]. However, again, instability conditions were not discussed in Ref. [13]. All of our attempts to formulate a theory with constraint to find polynomials (up to the tenth degree) in order to reproduce the proper PT criteria (which are known from two-phase treatment) from the thermodynamic instability conditions have been unsuccessful. This led us to the conclusion that utilizing constraint $\sum \eta_i = 1$ prevents a noncontradictory formulation of the PFA.

PFA in Ref. [3] is based on a potential in hyperspherical order parameters, in which one of the phases, O (e.g., A or melt), is at the center of the sphere, and all others, P_i (e.g., M_i or solid phases), are located at the sphere. Hyperspherical order parameters represent a radius Υ in the order-parameter space and the angles between radius vector $\boldsymbol{\Upsilon}$ and the axes η_i corresponding to P_i.

Due to some problems found in Ref. [14], the nonlinear constraint for the hyperspherical order parameters was substituted
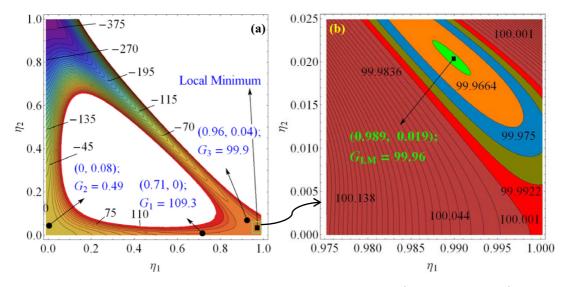

FIG. 1. (Color online) (a) Energy level plot of the free energy at zero stresses for $A_1 + 3\Delta G_1^\theta = 1000$, $A_1 - 3\Delta G_1^\theta = 400$, $A_2 + 3\Delta G_2^\theta = 230$, $A_2 - 3\Delta G_2^\theta = 2570$, $\bar{A} + A_1(\theta) + 3\Delta G_1^\theta = -250$, and $A_{21}(\theta) - 3G_{21}^\theta = 150$, all in J/m^3. G_i are the points of the local minimaxes. (b) The zoomed part of the plot near P_1.

with the linear constraint of the type $\sum \eta_i = 1$, which, however, does not include A or melt [12,14]. For three phases, when constraint is explicitly eliminated, the theory in Refs. [3,12,14] is completely consistent with the two-phase theory and produces proper PT criteria. However, due to the constraint, for more than three phases, these theories cannot produce correct PT criteria. Thus, noncontradictory PFA for more than three phases or two martensitic variants is currently lacking.

In this paper, we develop PFA, which with high and controllable accuracy satisfy all the desired conditions for arbitrary n phases. We utilize the same order parameters η_i like for martensitic PT and, instead of explicit constraints, include in the simplest potential the terms that penalize the deviation of the trajectory in the order parameter space from the straight lines connecting *each two phases*. These penalizing terms do not contribute to the instability conditions and the correct PT criteria strictly follow from the instability conditions for $O \leftrightarrow P_i$ PT only. However, when the magnitude of the penalizing term grows to infinity and imposes the strict constraint $\eta_i + \eta_j = 1$ and $\eta_k = 0$ for all $k \neq i, j$, correct PT conditions for $P_i \leftrightarrow P_j$ PTs do follow from the instability conditions, because for a finite magnitude such a constraint is applied approximately only, there is some deviation from the ideal equilibrium phases and PT conditions. However, numerical simulations for the almost worst cases demonstrate that these deviations are indeed negligible. This PFA allows for an analytical solution for the interfaces between each of the two phases, which can be used to calibrate interface width, energy, and mobility; it allows for the first time for a multiphase system to include a consistent expression for interface stresses for each interface; it includes or excludes the third phase within the interface between the two phases based on thermodynamic and kinetic considerations similar to those in Ref. [12].

We designate contractions of tensors $\boldsymbol{A} = \{A_{ij}\}$ and $\boldsymbol{B} = \{B_{ji}\}$ over one and two indices as $\boldsymbol{A} \cdot \boldsymbol{B} = \{A_{ij} B_{jk}\}$ and $\boldsymbol{A} : \boldsymbol{B} = A_{ij} B_{ji}$, respectively. The subscript s means symmetrization, the superscript T designates transposition, the sub- and superscripts e, th, and t mean elastic, thermal, and

transformational strains, $\boldsymbol{I}$ is the unit tensor, and $\boldsymbol{\nabla}$ and $\boldsymbol{\nabla}_0$ are the gradient operators in the *deformed* and undeformed states.

II. GENERAL MODEL

A. Model for *n* order parameters

For simplicity and compactness, the small strains will be considered but with some minimal geometric nonlinearities required to introduce interface stresses [5–7]. Generalization for large strain is straightforward, [4,5] and the model problem will be solved in large strain formulation. The Helmholtz free energy ψ per unit undeformed volume has the following form:

$$\psi = \frac{\rho_0}{\rho_t}\psi^e(\boldsymbol{\varepsilon}_e, \eta_i, \theta) + \frac{\rho_0}{\rho}\breve{\psi}^\theta + \tilde{\psi}^\theta + \frac{\rho_0}{\rho}\psi^\nabla + \psi_p, \quad (1)$$

$$\breve{\psi}^\theta = \sum A_i(\theta)\eta_i^2(1 - \eta_i)^2 + \sum \bar{A}_{ij}\eta_i^2 \eta_j^2, \quad (2)$$

$$\tilde{\psi}^\theta = \sum \Delta G_i^\theta(\theta)q(\eta_i); \quad q(\eta_i) = \eta_i^2(3 - 2\eta_i), \quad (3)$$

$$\psi_p = \sum K_{ij}(\eta_i + \eta_j - 1)^2\eta_i^l\eta_j^l + \sum K_{ijk}\eta_i^2\eta_j^2\eta_k^2, \quad l \geqslant 2, \quad (4)$$

$$\psi^e = 0.5\boldsymbol{\varepsilon}_e : \boldsymbol{E}(\eta_i) : \boldsymbol{\varepsilon}_e, \quad \boldsymbol{E}(\eta_i) = \boldsymbol{E}_0 + \sum(\boldsymbol{E}_i - \boldsymbol{E}_0)q(\eta_i), \quad (5)$$

$$\psi^\nabla = \sum 0.5\beta_{ij}\boldsymbol{\nabla}\eta_i \cdot \boldsymbol{\nabla}\eta_j, \quad (6)$$

$$\boldsymbol{\varepsilon} = (\boldsymbol{\nabla}_0\boldsymbol{u})_s = \boldsymbol{\varepsilon}_e + \boldsymbol{\varepsilon}_t + \boldsymbol{\varepsilon}_\theta, \quad \frac{\rho_0}{\rho} = 1 + \varepsilon_v,$$

$$\varepsilon_v = \boldsymbol{\varepsilon} : \boldsymbol{I}, \quad \frac{\rho_0}{\rho_t} = 1 + (\boldsymbol{\varepsilon}_t + \boldsymbol{\varepsilon}_\theta) : \boldsymbol{I}, \quad (7)$$

$$\boldsymbol{\varepsilon}_t = \sum \boldsymbol{\varepsilon}_{ti}q(\eta_i), \quad \boldsymbol{\varepsilon}_\theta = \boldsymbol{\varepsilon}_{\theta 0} + \sum(\boldsymbol{\varepsilon}_{\theta i} - \boldsymbol{\varepsilon}_{\theta 0})q(\eta_i). \quad (8)$$

Here θ is the temperature, $\mathbf{u}$ is the displacements, $\boldsymbol{\varepsilon}$ is the strain tensor, ΔG_i^θ is the difference in the thermal energy between P_i and O, A_i and $\bar{A}_{ij}$ are the double-well barriers between P_i and O and between P_i and P_j, ρ, ρ_0, and ρ_t are the mass densities in the deformed, undeformed, and stress-free states, respectively, β_{ij} are the gradient energy coefficients, and each coefficient, K_{ij}, $\bar{A}_{ij}$, and K_{ijk}, is equal to zero if two subscripts coincide. Despite small strain approximation, we keep some geometrically nonlinear terms (ρ_0/ρ_t, ρ_0/ρ, and gradient $\boldsymbol{\nabla}$ with respect to deformed state) in order to correctly reproduce interface and elastic stresses [5–7].

The application of the thermodynamic laws and linear kinetics (see, e.g., Refs. [5–7]) results in

$$\boldsymbol{\sigma} = \boldsymbol{\sigma}_e + \boldsymbol{\sigma}_{st}, \qquad \boldsymbol{\sigma}_e = \frac{\rho}{\rho_0} \frac{\partial \psi^e}{\partial \boldsymbol{\varepsilon}_e}, \qquad (9)$$

$$\boldsymbol{\sigma}_{st} = (\psi^\nabla + \breve{\psi}_\theta)\boldsymbol{I} - \sum \beta_{ij} \boldsymbol{\nabla}\eta_i \otimes \boldsymbol{\nabla}\eta_j, \qquad (10)$$

$$\dot{\eta}_i = \sum L_{ij} X_j = \sum L_{ij} \left[\boldsymbol{\sigma}_e : \frac{\partial(\boldsymbol{\varepsilon}_t + \boldsymbol{\varepsilon}_\theta)}{\partial \eta_j} - \frac{\partial \psi}{\partial \eta_j} \right.$$
$$\left. + \sum \beta_{jk} \boldsymbol{\nabla}^2 \eta_k \right], \quad L_{ij} = L_{ji}, \qquad (11)$$

where X_i is the thermodynamic driving force to change η_i, L_{ij} are the kinetic coefficients, and $\boldsymbol{\sigma}$ is the true Cauchy stress tensor. We designate the set of the order parameters $\hat{\eta}_0 = (0,\ldots,0)$ for O and $\hat{\eta}_i = (0,\ldots,\eta_i=1,\ldots,0)$ for P_i. It is easy to check that O and P_i are homogeneous solutions of the Ginzburg-Landau equations (11) for arbitrary stresses and temperature; consequently, the transformation strain and for any PT and elastic moduli are independent of stresses and temperature [2–4].

Without the term ψ_p, the local part of free energy is much simpler than in Refs. [2,3] and does not contain complex interaction between phases. The terms with K_{ijk} penalize the presence of the three phases at the same material point. By increasing K_{ijk} one can control and, in particular, completely exclude the third phase within the interface between the two other phases. For homogeneous states, this term always excludes the presence of the three phases at the same point, because it increases energy compared with a two-phase state. The terms with K_{ij} penalize deviations from hyperplanes $\eta_k = 0$ and $\eta_i + \eta_j = 1$, and exponent l determines relative weight of these penalties. In combination with the penalization of more than two phases, this constraint penalizes deviation from the desirable transformation paths: along coordinate lines η_i along which $O \leftrightarrow P_i$ PTs occur, and lines $\eta_i + \eta_j = 1$, $\eta_k = 0 \; \forall k \neq i,j$, along which $P_i \leftrightarrow P_j$ PTs occur. In such a way, we do not need to impose the explicit constraint $\sum \eta_i = 1$ and will be able to (approximately) satisfy all desired conditions, including instability conditions. Note that there is no need for penalizing $\eta_i = 0$; however, for $l = 0$ the term with K_{ij} produces an undesired contribution to ψ for $\eta_i = 0$.

B. Thermodynamic instability conditions

For compactness, instability conditions will be presented for the case with the same elastic moduli of all phases and $\rho_0 \simeq \rho$. Since $\partial X_i(\hat{\eta}_k)/\partial \eta_j = 0$, instability conditions for

thermodynamically equilibrium homogeneous phases result in the following PT criteria:

$$O \to P_i : \quad \partial X_i(\hat{\eta}_0)/\partial \eta_i \geqslant 0 \to \boldsymbol{\sigma}_e : (\boldsymbol{\varepsilon}_{ti} + \boldsymbol{\varepsilon}_{\theta i} - \boldsymbol{\varepsilon}_{\theta 0})$$
$$- \Delta G_i^\theta \geqslant A_i(\theta)/3, \qquad (12)$$

$$P_i \to O : \quad \partial X_i(\hat{\eta}_i)/\partial \eta_i \geqslant 0 \to \boldsymbol{\sigma}_e : (\boldsymbol{\varepsilon}_{ti} + \boldsymbol{\varepsilon}_{\theta i} - \boldsymbol{\varepsilon}_{\theta 0})$$
$$- \Delta G_i^\theta \leqslant -A_i(\theta)/3, \qquad (13)$$

$$P_j \to P_i : \quad \partial X_i(\hat{\eta}_j)/\partial \eta_i \geqslant 0 \to \boldsymbol{\sigma}_e : (\boldsymbol{\varepsilon}_{ti} + \boldsymbol{\varepsilon}_{\theta i} - \boldsymbol{\varepsilon}_{\theta 0})$$
$$- \Delta G_i^\theta \geqslant (A_i(\theta) + \bar{A})/3 \; \Rightarrow \; \text{wrong.} \qquad (14)$$

While conditions for $O \leftrightarrow P_i$ PTs are logical (work of stress on jump in transformation and thermal strains exceeds some threshold), the condition for $P_j \to P_i$ does not contain information about phase P_j, which is contradictory even at zero stresses. Since first and second derivatives of ψ_p are zero for O and P_i, ψ_p does not change phase equilibrium and instability conditions for homogeneous phases. However, as we will see below, it plays a key role in the development of noncontradictory and flexible PFA.

C. $O \leftrightarrow P_i$ phase transformations

If $O \leftrightarrow P_i$ PT is considered only with all other $\eta_j = 0$, Eqs. (2)–(6) simplify to

$$\breve{\psi}^\theta = A_i(\theta)\eta_i^2(1-\eta_i)^2, \quad \tilde{\psi}^\theta = \Delta G_i^\theta(\theta)q(\eta_i),$$
$$\psi_p = 0, \quad \psi^\nabla = 0.5\beta_{ii}\boldsymbol{\nabla}\eta_i \cdot \boldsymbol{\nabla}\eta_i, \qquad (15)$$

$$\boldsymbol{E}(\eta_i) = \boldsymbol{E}_0 + (\boldsymbol{E}_i - \boldsymbol{E}_0)q(\eta_i), \quad \boldsymbol{\varepsilon}_t = \boldsymbol{\varepsilon}_{ti}q(\eta_i),$$
$$\boldsymbol{\varepsilon}_\theta = \boldsymbol{\varepsilon}_{\theta 0} + (\boldsymbol{\varepsilon}_{\theta i} - \boldsymbol{\varepsilon}_{\theta 0})q(\eta_i), \qquad (16)$$

$$\boldsymbol{\sigma}_{st} = (\psi^\nabla + \breve{\psi}_\theta)\boldsymbol{I} - \beta_{ii}\boldsymbol{\nabla}\eta_i \otimes \boldsymbol{\nabla}\eta_i, \qquad (17)$$

$$\dot{\eta}_i = L_{ii}\left[\boldsymbol{\sigma}_e : (\boldsymbol{\varepsilon}_{ti} + \boldsymbol{\varepsilon}_{\theta i} - \boldsymbol{\varepsilon}_{\theta 0})\frac{dq}{d\eta_i} - \frac{\partial \psi}{\partial \eta_i} + \beta_{ii}\boldsymbol{\nabla}^2\eta_i \right]. \qquad (18)$$

These equations possess all desired properties [2–4] of two-phase models.

D. $P_j \leftrightarrow P_i$ phase transformations

Next, we consider how to make the description of $P_j \to P_i$ PTs completely similar to that of $O \leftrightarrow P_i$ PTs. Let us increase parameters K_{ij} and $\bar{K}_{ijk}$ to very high values so that they impose constraints $\eta_i + \eta_j = 1$ and $\eta_k = 0 \; \forall k \neq i,j$. Substituting these constraints in Eq. (1) and taking into account the following properties of function q, $q(1-\eta_i) = 1 - q(\eta_i)$ (which is crucial for our PFA), we reduce all equations to the single order parameter:

$$\breve{\psi}^\theta = A_{ij}(\theta)\eta_i^2(1-\eta_i)^2, \quad A_{ij} = A_i + A_j + \bar{A}_{ij}, \qquad (19)$$

$$\tilde{\psi}^\theta = \Delta G_j^\theta + \Delta G_{ij}^\theta(\theta)q(\eta_i), \quad \Delta G_{ij}^\theta = \Delta G_i^\theta - \Delta G_j^\theta, \qquad (20)$$

$$\boldsymbol{E} = \boldsymbol{E}_j + (\boldsymbol{E}_i - \boldsymbol{E}_j)q(\eta_i), \qquad (21)$$

$$\psi^\nabla = 0.5 b_{ij} \boldsymbol{\nabla}\eta_i \cdot \boldsymbol{\nabla}\eta_i, \quad b_{ij} = \beta_{ii} + \beta_{jj} - 2\beta_{ij}, \quad (22)$$

$$\boldsymbol{\varepsilon}_t = \boldsymbol{\varepsilon}_{tj} + (\boldsymbol{\varepsilon}_{ti} - \boldsymbol{\varepsilon}_{tj})q(\eta_i), \quad \boldsymbol{\varepsilon}_\theta = \boldsymbol{\varepsilon}_{\theta j} + (\boldsymbol{\varepsilon}_{\theta i} - \boldsymbol{\varepsilon}_{\theta j})q(\eta_i),$$
$$(23)$$

$$\boldsymbol{\sigma}_{st} = (\psi^\nabla + \check{\psi}_\theta)\boldsymbol{I} - b_{ij}\boldsymbol{\nabla}\eta_i \otimes \boldsymbol{\nabla}\eta_i,$$
$$l_{ij} = (L_{ii}L_{jj} - L_{ij}^2)/(L_{jj} + L_{ij}),$$
$$(24)$$

$$\dot{\eta}_i = l_{ij}\left[\boldsymbol{\sigma}_e{:}(\boldsymbol{\varepsilon}_{ti} + \boldsymbol{\varepsilon}_{\theta i} - \boldsymbol{\varepsilon}_{tj} - \boldsymbol{\varepsilon}_{\theta j})\frac{dq}{d\eta_i} - \frac{\partial\psi}{\partial\eta_i} + b_{ij}\boldsymbol{\nabla}^2\eta_i\right],$$
$$(25)$$

$$P_j \to P_i, \quad \partial X_i(\hat{\eta}_j)/\partial\eta_i \geqslant 0 \to \boldsymbol{\sigma}_e{:}(\boldsymbol{\varepsilon}_{ti} + \boldsymbol{\varepsilon}_{\theta i} - \boldsymbol{\varepsilon}_{tj} - \boldsymbol{\varepsilon}_{\theta j})$$
$$- \Delta G_{ij}^\theta \geqslant A_{ij}(\theta)/3. \quad (26)$$

It is evident that Eqs. (19)–(26) for $P_j \to P_i$ PTs are noncontradictory (i.e., contain an expected combination of parameters of P_j and P_i) and coincide to within constants and designations with Eqs. (15)–(18) for $O \leftrightarrow P_i$ PTs; i.e., they are as good as the equations for $O \leftrightarrow P_i$ PTs. Thus, our goal is achieved.

E. Energy landscape and $P_j \leftrightarrow P_i$ instability conditions for finite K_{ij}

Note that instability condition (26) works in the limit $K_{ij} \to \infty$; for finite K_{ij} it is imposed approximately only. To better understand the interaction between instability conditions (14) and (26), we consider some examples. We consider the case when PT conditions for $O \leftrightarrow P_i$ PTs [(12) and (13)] and for $P_j \to P_i$ PT (26) are not met, but when the wrong condition (14) is fulfilled with quite large deviation from the stability region. Under such conditions, P_j loses its stability, but instead of transforming to P_i, the local energy minimum slightly shifts from $\eta_1 = 1$, $\eta_2 = 0$ to a close point $\eta_1 = 0.989$, $\eta_2 = 0.019$ (Fig. 1). There is an energy barrier (saddle point) between P_j and P_i, and until it disappears [i.e., correct condition (26) for $P_j \to P_i$ PT is met], $P_j \to P_i$ PT is impossible. Thus, an approximate character of the imposed constraint through the penalty term exhibits itself in a slight shift of the local minimum from P_j to some very close point, which should essentially not affect the accuracy of the simulations.

If PT conditions for $O \leftrightarrow P_i$ PTs (13) and (14) are not fulfilled but the correct condition (26) for $P_j \to P_i$ PT is met, then these equations result in $\bar{A} < 0$. It is easy to show that in this case the wrong $P_j \to P_i$ PT condition (14) should be also fulfilled. Thus, if the correct $P_j \to P_i$ PT condition is met, this PT will occur.

III. PARAMETER IDENTIFICATION

Due to equivalence of all equations for $O \leftrightarrow P_i$ and $P_j \to P_i$ PTs, the analytical solution for a propagating with velocity c interface is [8]

$$\eta = 0.5\tanh[3(x - ct)/\delta] + 0.5, \quad \delta = \sqrt{18\beta/A_i(\theta)},$$
$$c = L\delta\Delta G^\theta(\theta), \quad \gamma = \beta/\delta, \quad (27)$$

where δ and γ are the interface width and energy. In contrast to solutions for other interpolating functions q [5–7], interface width and energy are independent of $\Delta G^\theta(\theta)$. That is why $\check{\psi}^\theta$ and interface stresses $\boldsymbol{\sigma}_{st}$ are also independent of $\Delta G^\theta(\theta)$. All material parameters for each bulk phase can be determined based on thermodynamic, experimental, and atomistic data as was done, e.g., in Refs. [2,3] for NiAl. Equations (27) allow calibration for each pair of phases the three interface-related parameters $A_i(\theta)$, β, and L when width, energy, and mobility of interfaces between each pair of phases are known.

The obtained system of equations has been solved with the help of the finite element code COMSOL for various problems. Here we solved exactly the same problem on the evolution of two-variant nanostructure in a NiAl alloy during martensitic PT including tip bending and splitting in martensitic variants as in Ref. [14]. Note that the theory in Ref. [14] for two variants satisfies all required conditions exactly but cannot be generalized for more than two variants. Some material parameters [like $\mathbf{E}, \boldsymbol{\varepsilon}_{ti}, \Delta G^\theta(\theta), \theta_e, \Delta s$] here have been chosen the same as in Ref. [14]; other [$A_{ij}(\theta), \beta_{ij}(\theta), L_{ij}, \theta_c$] are chosen to get the temperature dependence of the energy, width, and mobility of all interfaces, and temperature for the loss of stability of P like in Ref. [14]. Note that all thermodynamic properties of martensitic variants M_1 and M_2 are the same; they differ by the transformation strain only.

We have the following definition of parameters: $\Delta G_1^\theta = \Delta G_2^\theta = -\Delta s(\theta - \theta_e)$, where $\Delta s = s_i - s_0$ is the jump in entropy between phases M_i and A, and θ_e is the thermodynamic equilibrium temperature for phases T_i and A. We express the coefficients $A_1(\theta) = A_2(\theta) = A_*(\theta - \theta_*)$. Here parameter A_* and the characteristic temperature θ_* are related to the critical temperatures for barrierless $A \to P_i$ (θ_c^{0i}) and $P_i \to A$ (θ_c^{i0}) PTs by the equations $\theta_c^{01} := (A_*\theta_* - 3\Delta s\theta_e)/(A_* - 3\Delta s)$ and $\theta_c^{10} := (A_*\theta_* + 3\Delta s\theta_e)/(A_* + 3\Delta s)$, which follow from the thermodynamic instability conditions.

In the current simulation we used the following values: $\Delta s = -1.467 M$ Pa K^{-1}, $\theta_e = 215$ K, $\theta_c^{01} = -183$ K, $\theta_c^{10} = -331.65$ K, $\theta_* = -245.75$ K, $A_* = 28 M$ Pa K^{-1}, $\beta_{01} = \beta_{02} = 5.31 \times 10^{-10}$ N, $\beta_{12} = 5.64 \times 10^{-10}$ N, $L_{0i} = L_{12} = 2596.5$ m$^2/N$ s. These parameters correspond to a twin interface energy $E_{P_1 P_2} = 0.543$ J/m^2 and width $\Delta_{P_1 P_2} = 0.645$ nm. Isotropic linear elasticity was utilized for simplicity; bulk modulus $K = 112.8$ G Pa and shear modulus $\mu = 65.1$ G Pa. In the two-dimensional plane stress problems, only P_1 and P_2 are considered. The components of the transformation strains were $\mathbf{U}_{t1} = (k_1, k_2, k_2)$ and $\mathbf{U}_{t2} = (k_2, k_1, k_2)$ with $k_1 = 1.15$ and $k_2 = 0.93$ corresponding to the NiAl alloy in Ref. [15]. In addition, $K_{ijk} = 0$ and two values of $K_{12} = 1.5 \times 10^{12}$ and $K_{12} = 7.25 \times 10^{13}$ J/m^3 have been used. All lengths, stresses, and times are given in units of nm, GPa, and ps, respectively. All external stresses are normal to the deformed surface.

IV. EVOLUTION OF MARTENSITIC NANOSTRUCTURE

A. Numerical procedure

We used Lagrange quadratic triangular elements with five to six elements per interface width to achieve a mesh-independent solution; see Ref. [16]. This resulted in 165 601 mesh points and 329 760 elements with 1 982 883 degrees of freedom.
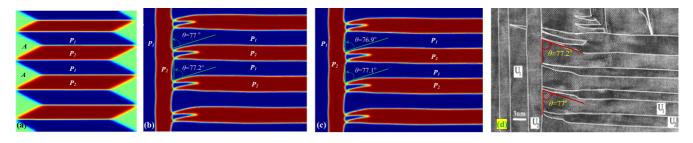
FIG. 2. (Color online) Initial conditions (a) and stationary solution for two-variant martensitic nanostructure exhibiting bending and splitting martensitic tips based on the current theory (b) and theory in Ref. [14] (c); experimental nanostructure from [15] (d). Green is for austenite, blue and red are for martensitic variants P_1 and P_2.

Adaptive mesh generation was utilized. The time-dependent equations were solved using the segregated time-dependent solver and backward Euler integration technique [17] for 250 ps. Integration time steps were chosen automatically such that a relative tolerance of 0.001 and absolute tolerance of 0.0001 are held.

B. Nanostructure

Because numerous alternative solutions exist, one has to carefully choose the initial conditions. We did this using the following steps. An initial random distribution of the order parameters η_1 and η_2 in the range [0.4; 0.8] were prescribed in a square sample sized 50×50 with the austenite lattice rotated by $\alpha = 45°$. The roller support was used for one horizontal and one vertical surface; i.e., the normal displacements and shear stresses are zero. Homogeneous normal displacements at two other surfaces were prescribed and kept constant during simulations, which resulted in a biaxial normal strain of 0.01. Shear stresses were kept zero at external surfaces. A two-dimensional problem under plane stress condition and temperature $\theta = 100$ K was solved. The stationary solution for $\theta = 100$ K shown in Fig. 2(a) (which is practically the same as presented in Ref. [14]) was taken as an initial condition for the next stage of simulation with the following modifications: temperature was reduced to $\theta = 0$ K, and parameter β_{12} was reduced to $\beta_{12} = 5.64 \times 10^{-11} N$, which led to twin interface energy $E_{P_1 P_2} = 0.371$ J/m^2 and width $\Delta_{P_1 P_2} = 0.363$ nm. The final solution evolution of $\eta_1 - \eta_2$ is presented in Fig. 2(b).

Results of the current simulations for both K_{12} practically coincide with those in Ref. [14] [Fig. 2(c)]; they resemble the experimental nanostructure from Ref. [15] and quantitatively reproduce the bending angle [Fig. 2(d)]. Thus, we proved that for two variants our theory does not work worse than the

theory, [14] which strictly satisfies all desired conditions for two variants. However, in contrast to Ref. [14], the current theory can be applied for an arbitrary number of variants. Since our theory splits the general n-phase case into a set of independent three-phase formulations, this means that it will work equally well for arbitrary n as well. An important point also is that such a complicated nanostructure was obtained from a completely different initial nanostructure [Fig. 2(a)]. For example, the splitting and bending of the tips were also reproduced in Ref. [18] utilizing strain-based phase-field formulation. However, the initial conditions in Ref. [18] were very close to the final solution, because probably otherwise the solution converges to the primitive alternating twins. Note that the strain-based order parameters are not as universal as η_i (e.g., they cannot be used for melting or grain evolution). and as was written in Refs. [2,3], they do not allow one to satisfy the required conditions even for a single order parameter. Interface stresses also were not introduced for strain-based order parameters.

C. Stresses

Components of the stress fields, including interface stresses, are shown in Fig. 3. They are seldom presented in literature because of large artificial oscillations. Here oscillations are absent, and stress concentration has a regular character, which underlines the advantages of the current simulations. Since twin boundaries represent invariant plane, it is generally assumed in a sharp interface approach that they are stress-free and do not generate elastic energy. Here we unexpectedly observe large shear stress σ_{xy}, which changes the sign across the twin interface. Shear stress appears due to the accommodation of large alternating shears across a finite-width interface in a constraint sample.
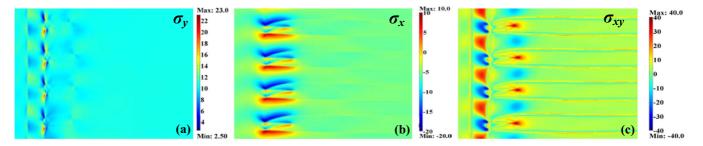

FIG. 3. (Color online) Stationary stress fields (in GPa) for $K_{12} = 1.5 \times 10^{12}$ J/m^3.

V. CONCLUDING REMARKS

To summarize, as a solution of a critical outstanding problem, we developed PFA for multiphase materials, which with high and controllable accuracy satisfy all the desired conditions for arbitrary n phases. Instead of explicit constraints, we included in the simplest potential the terms that penalize the deviation of the trajectory in the order parameter space from the straight lines connecting each of the two phases. It describes each of the PTs with the single order parameter, which allows us to use an analytical solution to calibrate each interface energy, width, and mobility. It reproduces the desired PT criteria via instability conditions, introduces interface stresses, and allows us to control the presence of the third phase at the interface between the two other phases. Finite-element simulations exhibit very good correspondence with results based on the exact three-phase model in Ref. [14] (which,

however, cannot be generalized for $n > 3$) and with nontrivial experimental nanostructure. The developed approach unifies and integrates approaches developed in different communities (in particular, solidification and martensitic PTs) and is applicable to various PTs between multiple solid and liquid phases and grain evolution and can be extended for diffusive, electric, and magnetic PTs.

[1] A. Artemev, Y. Jin, and A. G. Khachaturyan, Three-dimensional phase field model of proper martensitic transformation, Acta Math. **49**, 1165 (2001); Y. M. Jin, A. Artemev, and A. G. Khachaturyan, Three-dimensional phase field model of low-symmetry martensitic transformation in polycrystal: simulation of ζ_2' martensite in AuCd alloys, *ibid.* **49**, 2309 (2001); L.-Q. Chen, Phase-field models for microstructure evolution, Annu. Rev. Mater. Res. **32**, 113 (2002); Y. Wang and A. G. Khachaturyan, Multi-scale phase field approach to martensitic transformations, Mat. Sci. Engg. A **438-440**, 55 (2006); M. Mamivand, M. A. Zaeem, and H. El Kadiri, A review on phase field modeling of martensitic phase transformation, Comp. Mat. Sci. **77**, 304 (2013).

[2] V. I. Levitas and D. L. Preston, Three-dimensional Landau theory for multivariant stress-induced martensitic phase transformations. I. Austenite ↔ martensite, Phys. Rev. B **66**, 134206 (2002); Three-dimensional Landau theory for multivariant stress-induced martensitic phase transformations. II. Multivariant phase transformations and stress space analysis, **66**, 134207 (2002).

[3] V. I. Levitas, D. L. Preston, and D.-W. Lee, Three-dimensional Landau theory for multivariant stress-induced martensitic phase transformations. III. Alternative potentials, critical nuclei, kink solutions, and dislocation theory, Phys. Rev. B **68**, 134201 (2003).

[4] V. I. Levitas, V. A. Levin, K. M. Zingerman, and E. I. Freiman, Displacive Phase Transitions at Large Strains: Phase-Field Theory and Simulations, Phys. Rev. Lett. **103**, 025702 (2009); V. I. Levitas, Phase-field theory for martensitic phase transformations at large strains, Int. J. Plast. **49**, 85 (2013).

[5] V. I. Levitas, Phase field approach to martensitic phase transformations with large strains and interface stresses, J. Mech. Phys. Solids **70**, 154 (2014).

[6] V. I. Levitas, Interface stress for nonequilibrium microstructures in the phase field approach: Exact analytical result, Phys. Rev. B **87**, 054112 (2013); Thermodynamically consistent phase field approach to phase transformations with interface stresses, Acta Mater. **61**, 4305 (2013).

[7] V. I. Levitas and M. Javanbakht, Surface tension and energy in multivariant martensitic transformations: Phase-field theory, simulations, and model of coherent interface, Phys. Rev. Lett. **105**, 165701 (2010); V. I. Levitas, Unambiguous Gibbs dividing surface for nonequilibrium finite-width interface: Static equivalence approach, Phys. Rev. B **89**, 094107 (2014).

[8] I. Steinbach, F. Pezzolla, B. Nestler, M. Seeßelberg, R. Prieler, G. J. Schmitz, and J. L. L. Rezende, A phase field concept for multiphase systems, Physica D **94**, 135 (1996); I. Steinbach, Phase-field models in materials science, Model. Simul. Mater. Sci. Eng. **17**, 073001 (2009).

[9] H. Garcke, B. Nestler, and B. Stoth, On anisotropic order parameter models for multi-phase systems and their sharp interface limits, Physica D **115**, 87 (1998); R. Kobayashi and J. A. Warren, Modeling the formation and dynamics of polycrystals in 3D, Physica A **356**, 127 (2005); G. I. Tóth, J. R. Morris, and L. Gránásy, Ginzburg-Landau-type multiphase field model for competing fcc and bcc nucleation, Phys. Rev. Lett. **106**, 045701 (2011); G. I. Tóth, T. Pusztai, G. Tegze, G. Tóth, and L. Gránásy, Amorphous nucleation precursor in highly nonequilibrium fluids, *ibid.* **107**, 175702 (2011); Y. Mishin, W. J. Boettinger, J. A. Warren, and G. B. McFadden, Thermodynamics of grain boundary premelting in alloys. I. Phase-field modeling, Acta Mater. **57**, 3771 (2009).

[10] R. Folch and M. Plapp, Towards a quantitative phase-field model of two-phase solidification, Phys. Rev. E **68**, 010602 (2003); Quantitative phase-field modeling of two-phase growth, **72**, 011602 (2005).

[11] V. I. Levitas, B. F. Henson, L. B. Smilowitz, and B. W. Asay, Solid-solid phase transformation via virtual melting significantly below the melting temperature, Phys. Rev. Lett. **92**, 235702 (2004); V. I. Levitas, Z. Ren, Y. Zeng, Z. Zhang, and G. Han, Crystal-crystal phase transformation via surface-induced virtual premelting, Phys. Rev. B **85**, 220104 (2012).

[12] V. I. Levitas and K. Momeni, Solid-solid transformations via nanoscale intermediate interfacial phase: Multiple structures, scale and mechanics effects, Acta Mater. **65**, 125 (2014); K. Momeni and V. I. Levitas, Propagating phase interface with

intermediate interfacial phase: Phase field approach, Phys. Rev. B **89**, 184102 (2014); K. Momeni, V. I. Levitas, and J. A. Warren, The strong influence of internal stresses on the nucleation of a nanosized, deeply undercooled Melt at a solid-solid phase interface, Nano Lett. **15**, 2298 (2015).

[13] P. C. Bollada, P. K. Jimack, and A. M. Mullis, A new approach to multi-phase formulation for the solidification of alloys, Physica D **241**, 816 (2012).

[14] V. I. Levitas, A. M. Roy, and D. L. Preston, Multiple twinning and variant-variant transformations in martensite: Phase-field approach, Phys. Rev. B **88**, 054113 (2013).

[15] D. Schryvers, Ph. Boullay, R. V. Kohn, and J. M. Ball, Lattice deformations at martensite-martensite interfaces in Ni-Al, J.

de Physique IV **11**, 23 (2001); Ph. Boullay, D. Schryvers, and R. V. Kohn, Bending martensite needles in $Ni_{65}Al_{35}$ investigated by two-dimensional elasticity and high-resolution transmission electron microscopy, Phys. Rev. B **64**, 144105 (2001).

[16] V. I. Levitas and M. Javanbakht, Phase-field approach to martensitic phase transformations: Effect of martensite-martensite interface energy, Int. J. Mat. Res. **102**, 652 (2011).

[17] COMSOL, Inc., website: www.comsol.com.

[18] A. Finel, Y. Le Bouar, A. Gaubert, and U. Salman, Phase field methods: Microstructures, mechanical properties and complexity, C. R. Phys. **11**, 245 (2010).